

# Fluoride Salt Corrosion and Mass Transfer in High Temperature Dynamic Systems<sup>★</sup>

J. W. KOGER\*

## Abstract

Corrosion tests ranging from 3000 to 20,000 hours were conducted on nickel and iron based alloys in fused fluoride salt at temperatures ranging from 450 to 704 C (842 to 1299 F). The objective of the experiment was to find suitable fused salt container material for application in the nuclear molten salt reactor. The materials tested were Hastelloy N, titanium modified Hastelloy N, Type 304L stainless steel, and a maraging steel. The two types of salts were (1) LiF-BeF<sub>2</sub> with varying amounts of UF<sub>4</sub>, ThF<sub>4</sub>, and ZrF<sub>4</sub>, (fuel salt), and (2) a mixture of NaBF<sub>4</sub> and NaF (coolant salt). The compatibilities of these materials with the salts were determined from weight change data and chemical, metallographic, and electron microprobe analyses of the test specimens along with chemical analyses of the salts. The corrosion was manifested as temperature gradient mass transfer. The rate of corrosion of Hastelloy N in LiF-BeF<sub>2</sub> base salts was controlled by diffusion of chromium in the alloy and was very small (<0.1 mpy at 704 C), but the attack of stainless steel by the fuel salt was larger [1.1 mpy at 688 C (1270 F)]. Hastelloy N in NaBF<sub>4</sub>-NaF showed a uniform attack [0.6 mpy at 607 C (1125 F)] controlled by impurity reactions. A titanium modified Hastelloy N with no iron showed smaller weight changes than standard Hastelloy N with 5% Fe under similar conditions in a fuel salt. A maraging steel with less chromium than stainless steel had a corrosion rate half that of the stainless steel under similar conditions in a fuel salt.

Properties and corrosion characteristics of fluoride salts have been studied<sup>1</sup> since the early 1950's, first as a part of the Aircraft Nuclear Propulsion (ANP) Program and later in the development of the highly successful Molten Salt Reactor Experiment (MSRE).

Because of their radiation stability and their ability to contain both thorium and uranium in solution, mixtures of molten fluorides provide an effective fuel medium for high temperature fluid fuel reactor systems. They also have adequate heat transfer properties so they can be used as coolants. A variety of container materials, notably nickel base alloys, have proven compatible with certain of the fluoride salts, and Hastelloy<sup>(1)</sup> N was used in the MSRE. Nevertheless, at the high operating temperatures desired to achieve the inherent thermodynamic efficiencies of fused salt systems, the integration of fuel salt and coolant salts with moderator, structural, and control components into an amenable reactor complex presents more complex materials problems. Probably the most damaging type of corrosion that may occur is temperature gradient mass transfer (Figure 1). By this process, material oxidized and transferred from one portion of the system to another (usually from regions of high temperature to regions of lower temperature) may form plugs, thereby reducing and eventually stopping flow. This can take place before perceptible loss of material occurs in any one section. Thus, there has been an emphasis on the understanding of the corrosion

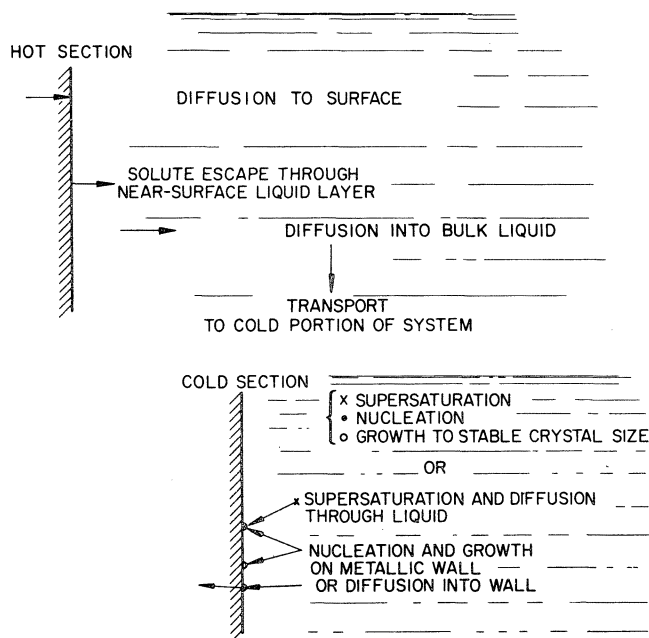


FIGURE 1 — Temperature gradient mass transfer.

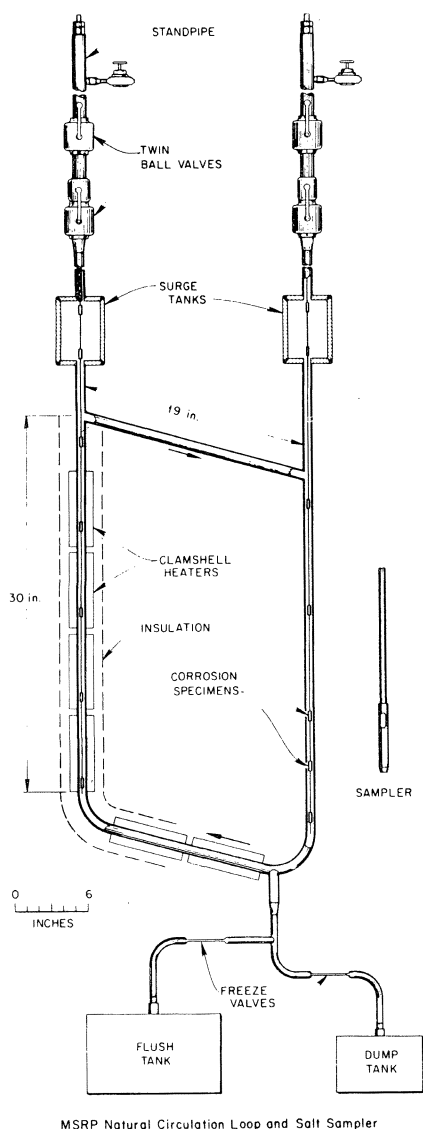
mechanism of these fused salts so that mass transfer can be predicted and perhaps controlled and failure of all parts of the system can be averted.

With the proposed use of other salt mixtures and changes in alloy composition, corrosion studies have continued, with the objective of this investigation being to determine the corrosion and mass transfer characteristics of salts proposed for use in the Molten Salt Breeder Reactor (MSBR). Variables included in the study are alloy composition, temperature, salt type, and impurity level of the salt.

\*Submitted for publication October, 1972. Research was sponsored by the U. S. Atomic Energy Commission under contract with the Union Carbide Corporation.

\*Metals and Ceramics Division, Oak Ridge National Laboratory, Oak Ridge, TN

<sup>(1)</sup> Tradename, Stellite Division of Cabot Corporation.



MSRP Natural Circulation Loop and Salt Sampler

FIGURE 2 — Natural circulation loop and salt sampler.

TABLE 2 — Alloy Compositions

Alloy	Cr	Content, %		
		Fe	Mo	Ni
Standard Hastelloy N	7.4	4.5	17.2	70.0
Ti-modified Hastelloy N	7.3	< 0.1	13.6	77.0
Type 304L stainless steel	18.3	68.0	< 0.1	10.1
Maraging steel <sup>(1)</sup>	5.0	80.0	3.0	12.0

(1) Nominal.

### Experimental Procedure and Materials

The tests were conducted in thermal convection loops, small scale dynamic systems that allow the investigation of mass transfer effects. A schematic view of a typical test unit is shown in Figure 2. The loops consisted of 1.9 cm OD x 1.54 cm ID tubing with 8.26 cm ID surge tanks atop each leg. Salt velocity ranged from 1 to 2 cm/sec, depending on the salt properties and the temperature gradient. The salt volume was 1300 cm<sup>3</sup>.

The loops were filled with salt from a fill tank by an applied helium pressure differential. The salt was prepared and purified by the Fluoride Processing Group of the Reactor Chemistry Division at Oak Ridge National Laboratory. An initial salt charge was used to remove surface oxides and other impurities. This salt was dumped after 24 hours in the loop, and the test salt was added. The hot portion of each loop was heated by clamshell heaters, while the cold leg and surge tanks were heated by tubular electric heaters. After the loop was filled, heat to the cold leg was turned off, and insulation was removed to induce flow and to obtain the desired temperature gradient. The flow resulted from the difference in density of the salt in the hot and cold portion of the loops.

Each corrosion test loop contained 14 specimens, 7 in each leg. Hastelloy N specimens were used in Hastelloy N loops and the iron base specimens in a Type 304L stainless steel loop. This minimized any dissimilar alloy corrosion effects. The salt compositions and specimen materials are

TABLE 1 — Materials and Salts in Corrosion Testing

Salt	Specimen Material	Salt Type
LiF-BeF <sub>2</sub> -ThF <sub>4</sub> (73-2-25 mole %)	Hastelloy N Ti-modified Hastelloy N	Fuel-fertile (two-fluid MSBR)
LiF-BeF <sub>2</sub> -UF <sub>4</sub> (65.5-34-0.5 mole %)	Hastelloy N Ti-modified Hastelloy N	Fuel-fissile (two-fluid MSBR)
LiF-BeF <sub>2</sub> -ThF <sub>4</sub> -UF <sub>4</sub> (68-20-11.7-0.3 mole %)	Hastelloy N Ti-modified Hastelloy N	Fuel-fertile-fissile (one-fluid MSBR)
NaBF <sub>4</sub> NaF (92-8 mole %)	Hastelloy N Ti-modified Hastelloy N	Coolant (MSBR)
LiF-BeF <sub>2</sub> -ZrF <sub>4</sub> -ThF <sub>4</sub> -UF <sub>4</sub> (70-23-5-1-1 mole %)	Type 304L stainless steel Maraging steel	Fuel (MSRE)

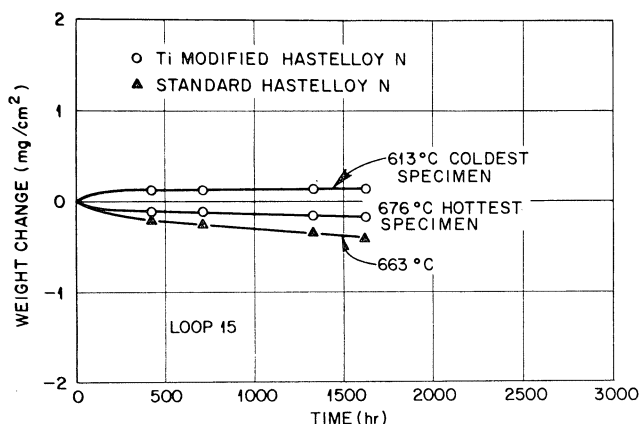


FIGURE 3 — Weight changes of Hastelloy N alloys in  $\text{LiF-BeF}_2\text{-ThF}_4$  (73.2-25 mole %).

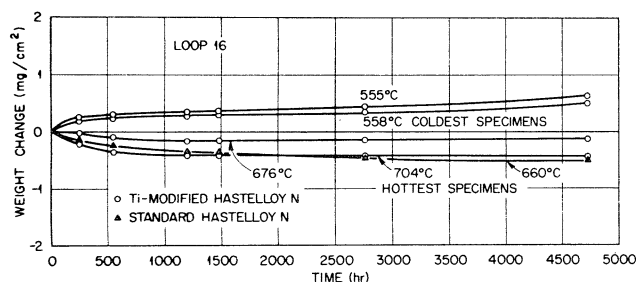


FIGURE 4 — Weight changes of Hastelloy N alloys in  $\text{LiF-BeF}_2\text{-UF}_4$  (65.5-34.0.5 mole %).

given in Table 1. The salts containing  $\text{UF}_4$  and/or  $\text{ThF}_4$  will be called fuel salts, and the  $\text{NaBF}_4\text{-NaF}$  salt will be called the coolant salt for purposes of discussion. The alloy compositions are given in Table 2. The titanium modified Hastelloy N was developed for improved radiation stability. The stainless and maraging steels were included to provide data on iron base systems. Weight change measurements, metallography, electron microprobe analyses, and chemical analyses were used to monitor the corrosion.

The test specimens were  $1.9 \times 0.95 \times 0.076$  cm. They were measured to within 0.0025 cm to obtain surface areas. They were triply weighed to within 0.01 mg and attached by wires to the specimen fixture, which consisted of 0.32 cm diameter rod welded to 0.63 cm OD tubing of the same material as the loop tubing. Salt for analysis was dip sampled from the harp portion of the loop into a hydrogen fired copper container attached to 0.63 cm OD copper tubing. Both the specimen fixture and the copper salt sampler were lowered into the loop through standpipes. The standpipes consisted of 1.0 inch (2.54 cm) sched 40 Type 304L stainless steel pipe with a 1.9 cm ball valve on one end and a Conax<sup>(2)</sup> fitting at the other through which the 0.63 cm OD tubing extended. Before they were opened to the loop environment, the standpipes were evacuated and backfilled with helium. On removal the specimen fixture or salt sample was pulled into the standpipe, isolated from the loop, and allowed to cool to room temperature. After salt

exposure and removal from the specimen fixture, the specimens were washed in warm water and then ethyl alcohol and dried. They were again triply weighed to within 0.01 mg, and the weight change was calculated. Salt samples were analyzed by the Analytical Chemistry Division of Oak Ridge National Laboratory.

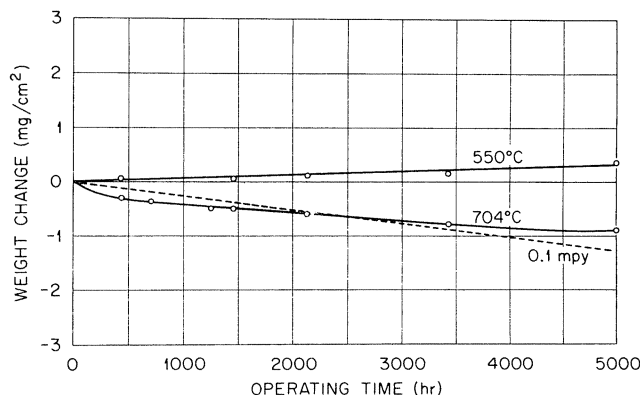


FIGURE 5 — Weight changes of Hastelloy N in  $\text{LiF-BeF}_2\text{-UF}_4\text{-ThF}_4$  (68.20-11.7-0.3 mole %).

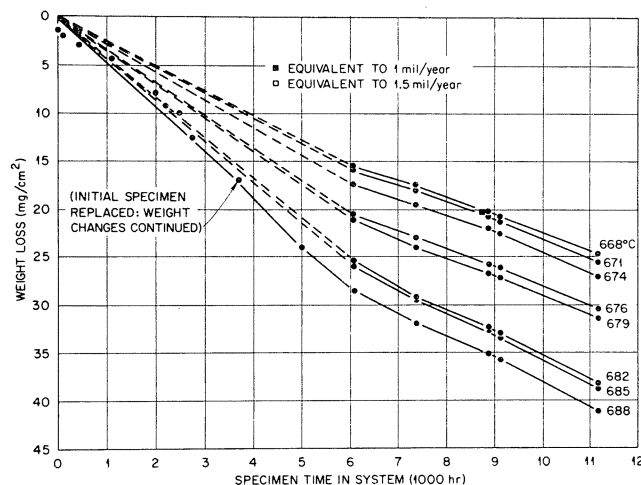


FIGURE 6 — Weight changes of Type 304 L stainless steel specimens in  $\text{LiF-BeF}_2\text{-ZrF}_4\text{-ThF}_4\text{-UF}_4$  (70.23-5.1-1 mole %).

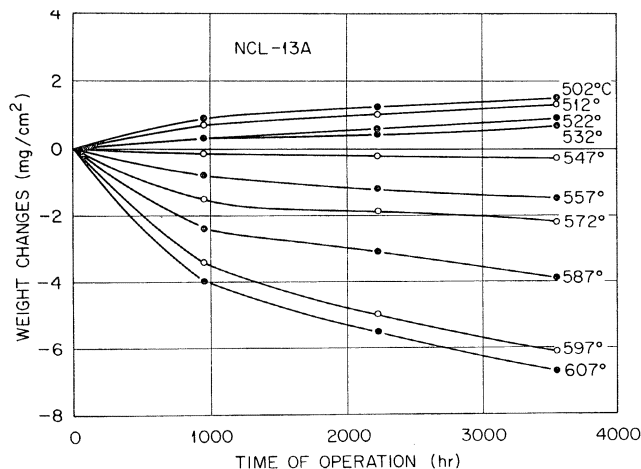


FIGURE 7 — Weight changes of standard Hastelloy N in  $\text{NaBF}_4\text{-NaF}$  (92.8 mole %).

<sup>(2)</sup> Tradename, Control Equipment Company, Inc.



**TABLE 3 — Comparison of Weight Losses of Alloys at About 663 C after 3730 Hours in Similar Flowing Fuel Salts in a Temperature Gradient**

Alloy	Weight Loss (mg/cm <sup>2</sup> )	Average Corrosion Rate (mpy)
Maraging steel	4.8	0.55
Type 304L stainless steel	10.0	1.10
Standard Hastelloy N	0.6	0.06

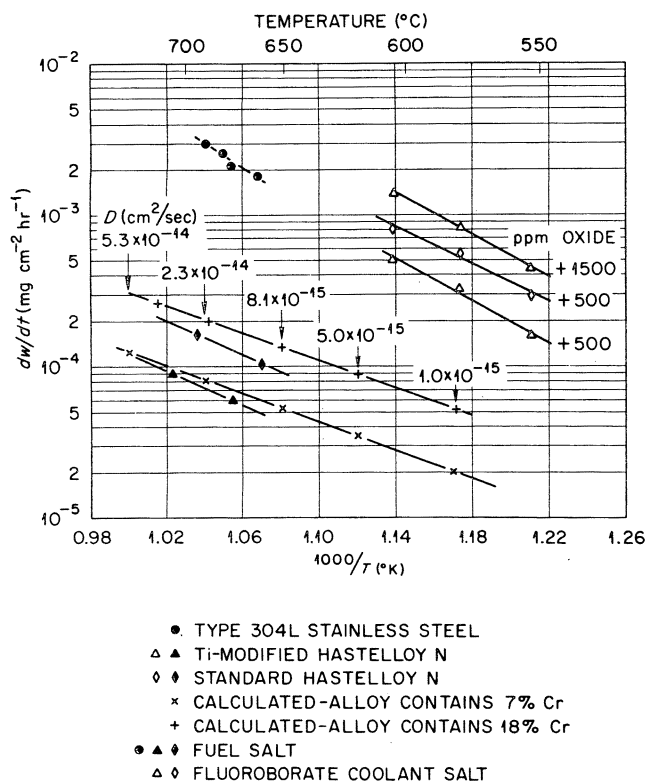


**FIGURE 8 — Arrhenius type plot for materials in fluoride salts.**

## Experimental Results

### Weight Change Data

The weight change data for the various tests are given in Figures 3 to 7 as functions of operating time. Losses as well as gains are indicated in most figures. For the fuel salt Hastelloy N system, Figures 3 to 5 show that the weight changes were quite small (<0.1 mpy at 704 C, assuming uniform loss) and that titanium modified specimens had smaller weight losses than standard Hastelloy N specimens, even though the standard specimens were exposed at lower temperatures. The weight changes are larger in Figures 6 and 7 (fuel salt-iron base alloys and coolant salt Hastelloy N systems, respectively), and assuming uniform loss, a corrosion rate of 1.1 mpy at the maximum temperature of 688 C was found for the stainless steel system (Figure 6) and 0.6 mpy at 607 C for the fluoroborate salt system (Figure 7). Table 3 compares weight losses of the maraging steel and stainless steel in identical environments along with

Hastelloy N under similar conditions. The maraging steel specimen shows one half the weight loss of the corresponding stainless specimen but still does not compare favorably to the Hastelloy N.

The average weight change per unit time for each system was calculated and is shown as a function of temperature in Figure 8. Also shown in this figure are weight changes calculated<sup>2</sup> from

$$\Delta W = 2\rho\Delta C\sqrt{Dt/\pi},$$

where

$\rho$  = density,

$\Delta C$  = change in chromium concentration from the bulk to the surface,

$D$  = diffusion coefficient for chromium, and

$t$  = time.

This equation is used to determine the total amount of material that diffuses from an alloy held under isothermal conditions with a zero surface concentration. The points on the calculated curves in Figure 8 were obtained by using chromium solid state diffusion coefficients<sup>3</sup> and assuming removal of only chromium. The data for Hastelloy N fuel salt systems do fit quite well, but the data for Hastelloy N

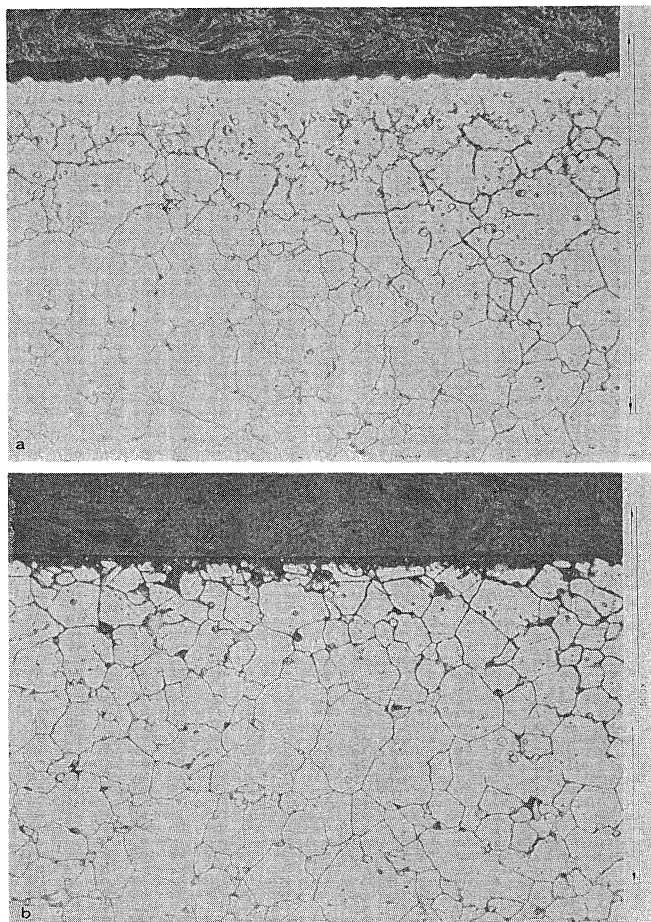


**FIGURE 9 — Microstructure of Hastelloy N exposed to LiF-BeF<sub>2</sub>-UF<sub>4</sub> (65.5-34-0.5 mole %) for 10,700 hours (a) 650 C, weight loss 1.3 mg/cm<sup>2</sup>, and (b) 550 C, weight gain 0.1 mg/cm<sup>2</sup>.**

in NaBF<sub>4</sub>-NaF and stainless steel in fuel salt indicate that a mechanism other than solid state diffusion may control the corrosion in those systems.

Salt Analysis

The major impurity concentration changes noted in the LiF-BeF<sub>2</sub> base salts exposed to Hastelloy N and stainless steel are chromium increases and eventual iron decreases. Iron increased initially in the stainless steel system. Increases in all the alloy constituent impurities were seen in NaBF<sub>4</sub>-NaF at the beginning of the test run. In time, the iron, nickel, and molybdenum contents decreased and the chromium content increased.

Typical microstructures of hot and cold leg specimens (Hastelloy N) from the LiF-BeF<sub>2</sub> base salts are shown in Figure 9. The alloys showed little surface modification and no measurable dimensional change. Voids formed in the stainless steel and maraging steel specimens of Figure 10. Little change in microstructure was seen for Hastelloy N specimens exposed to NaBF<sub>4</sub>-NaF (Figure 11). However, there were measurable dimensional changes. This is ascribed to the general type of corrosion attack seen in this system (as opposed to selective constituent removal).

Specimen Analysis

Electron microprobe and fluorescence analyses of Hastelloy N hot leg specimens exposed to the LiF-BeF<sub>2</sub> base salts show a decrease in the surface concentration of

TABLE 4 — Microprobe Analysis of Hastelloy N Specimen in Coldest Position (460 C) Exposed to Fluoroborate Salt for 4000 Hours

Element	Composition <sup>(1)</sup> wt %	
	Matrix	Deposit <sup>(2)</sup>
Ni	73.7	34.8
Mo	14.3	30.6
Cr	6.8	<0.5
Fe	3.8	2.9
Undetermined		≈ 33

(1) Corrected for absorption, secondary fluorescence, and atomic number effects.  
(2) Thin layer close to sample surface.

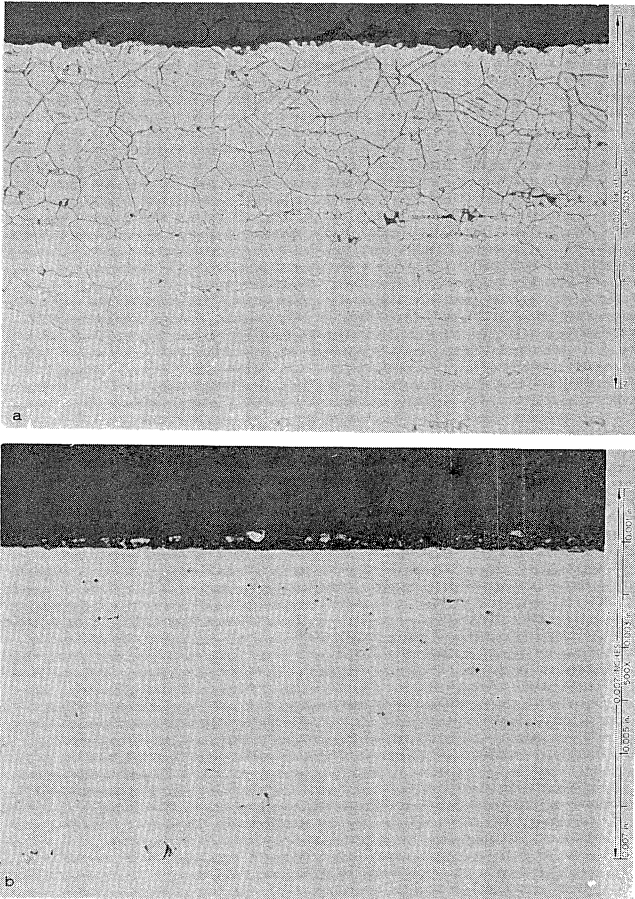


FIGURE 11 — Hastelloy N exposed to NaBF<sub>4</sub>-NaF (92-8 mole %). (a) Hot leg, 607 C, and (b) cold leg, 460 C.

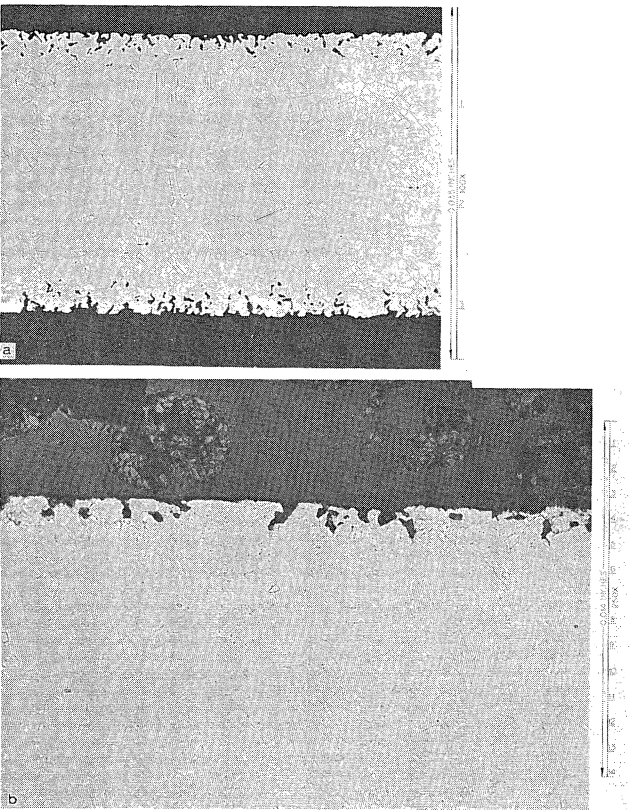


FIGURE 10 — Steels exposed to LiF-BeF<sub>2</sub>-ZrF<sub>4</sub>-UF<sub>4</sub>-ThF<sub>4</sub> (70-23-5-1-1 mole %) at 687 C. (a) Type 304L stainless steel, corrosion rate 1.1 mpy, and (b) maraging steel [Fe-12 Ni-5 Cr-3 Mo (weight %)], corrosion rate 0.55 mpy.

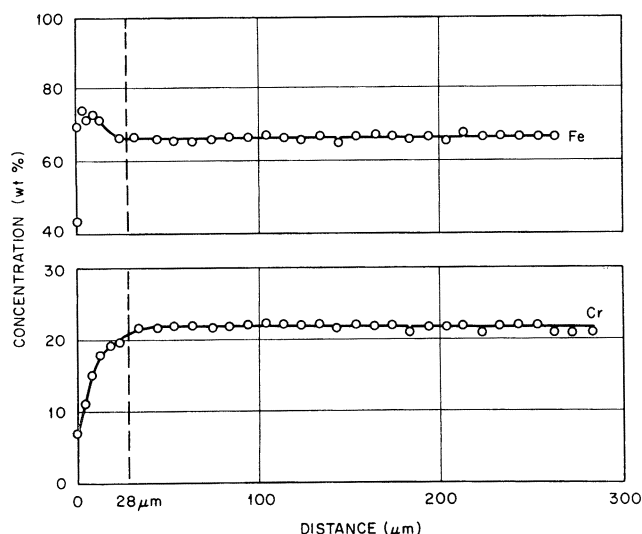
chromium with an increase in the surface concentration of iron. Chromium and iron gradients into the surface exist, but are too small to resolve.

Figure 12 shows the chromium and iron distribution for the stainless steel. No gross compositional changes were observed in the hot leg for the Hastelloy N subjected to NaBF<sub>4</sub>-NaF; however, the material deposited in the cold leg (Table 4) consisted mostly of nickel and molybdenum.

Discussion of Results

In general, the data show that weight changes (both





**FIGURE 12 – Chromium and iron gradients in Type 304L stainless steel exposed to LiF-BeF<sub>2</sub>-ZrF<sub>4</sub>-UF<sub>4</sub>-ThF<sub>4</sub> (70-23-5-1-1 mole %).**

**TABLE 5 – Relative Thermodynamic Stabilities of Fluorides**

Element	Most Stable Fluoride	Standard Free Energy of Formation per Gram Atom of Fluorine <sup>(1)</sup> (kcal/g-atom of F)	
		800 C	600 C
Structural Metals			
Cr	CrF <sub>2</sub>	-72	-77
Fe	FeF <sub>2</sub>	-66	-69
Ni	NiF <sub>2</sub>	-59	-63
Mo	MoF <sub>5</sub>	-57	-58
Molten Salt Components			
Li	LiF	-120	-125
Na	NaF	-110	-115
K	KF	-108	-113
Be	BeF <sub>2</sub>	-103	-100
Zr	ZrF <sub>4</sub>	-92	-96
B	BF <sub>3</sub>	-86	-88
Active Salts			
U	UF <sub>4</sub>	-92	-94
U	UF <sub>3</sub>	-93	-96
Th	ThF <sub>4</sub>	-99	-102

(1) A. Glassner. The Thermochemical Properties of the Oxides, Fluorides, and Chlorides to 2500 K, ANL-5750 (1957).

losses and gains) were functions of temperature. Also, balance points existed such that weight losses occurred above and weight gains below the temperature of the balance point. Thus, temperature-gradient mass transfer did occur. Salt analyses and microprobe data indicate mostly chromium movement in the alloys.

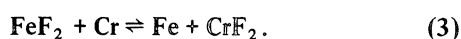
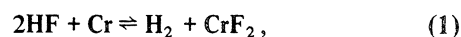
Table 5 lists the standard free energies of formation per gram atom of fluorine at 800 and 600 C (1472 and 1112 F) for various fluorides.<sup>4</sup> It appears from the free energies (assuming unit activities) that none of the salt constituents

can react with any of the alloy constituents. It also can be seen that of all the alloying constituents, chromium forms the most stable fluoride; it is the least noble.

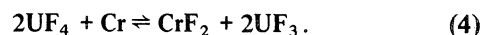
However, it must be kept in mind, as illustrated from an electrochemical viewpoint, that a metal will be oxidized if its potential in a melt is appreciably below the redox potential of the melt. On this basis, if one considers chromium (or iron or nickel) in a high purity LiF melt, corrosion can be expected until sufficient Cr<sup>2+</sup> ions have been produced by the oxidation of the metal to raise the potential of chromium to the same value as the redox potential of the melt. This will have been effected by the production of lithium metal by the cathodic reaction. It can be shown that there is one common potential for equilibrium, and the system will tend toward it during an experiment. The amount of material reacted in this case is quite small, but a finite activity of metal ions in the salt is required for equilibrium. If this is the only source of corrosion the systems are quite compatible. Again, this is only considering the thermodynamics and not the kinetics.

Several possible corrosion reactions of an actual system are listed below:

1. Impurities in the melt.



2. Added special constituents.



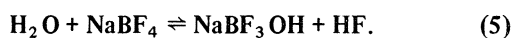
In each case, chromium is selectively oxidized. The attack by salts containing impurities and UF<sub>4</sub> is selective toward the alloying element (chromium in Hastelloy N or stainless steel) that forms the most stable fluoride. The rate is generally controlled by the diffusion rate of this element in the alloy. The corrosion reaction of UF<sub>4</sub> with chromium, Equation (4), has an equilibrium constant with a small temperature dependence; hence, when the salt is forced to circulate through a temperature gradient, a mechanism exists for mass transfer and continued attack. In theory, since the equilibrium constant for the chemical reaction increases with increasing temperature, the chromium concentration in the alloy surface would decrease at high temperature, resulting in a weight loss and increase at low temperature resulting in a weight gain. An intermediate temperature would exist at which the initial surface composition is in equilibrium with salt and no weight changes occur (balance point).

However, reactions of impurities such as metal fluorides or HF with the constituents of the alloys are possible, as can be seen by the negative free energies of formation. In extremely oxidizing conditions all the alloying elements are oxidized and the attack becomes uniform. Even in these cases the weight changes can still be a function of temperature. As mentioned earlier, weight losses and weight gains, in the hot and cold legs, respectively, and balance points were found in all these experiments,

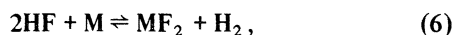
attesting to the temperature gradient mass transfer mechanism. It is also noteworthy to mention that mass transfer was not extensive enough in any of the systems to cause plugging or serious material depletion.

Hastelloy N responded differently to the two salts tested. It was quite compatible with the LiF-BeF<sub>2</sub> base salt, but exhibited measurable corrosion when exposed to the NaBF<sub>4</sub>-NaF salt. Only UF<sub>4</sub> of the major salt constituents will react to any extent with the alloying elements of Hastelloy N. As for impurities, both the fuel and coolant salts contained iron fluorides. However, there was one notable difference: the NaBF<sub>4</sub>-NaF salt contained over 500 ppm H<sub>2</sub>O and O<sub>2</sub>, as opposed to less than 100 ppm in the LiF-BeF<sub>2</sub> base salts. The effect of water-oxygen impurities will be discussed below.

A large part of the corrosion that occurs in fluoroborate salts is due to impurities, particularly moisture. One of the proposed corrosion reactions that involves water and fluoroborate is



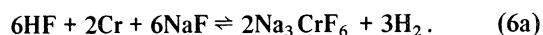
The reaction between HF and metal is



where

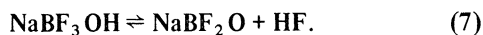
M = Cr, Fe, Ni, or Mo.

In our specific case, Equation (6) becomes

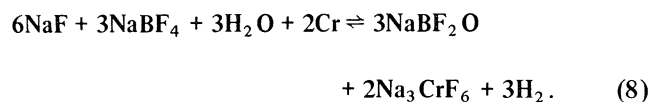


The effect of HF in a salt system can be quite virulent. A previous Hastelloy N loop circulating equimolar NaF-ZrF<sub>4</sub> salt saturated with HF operated only 200 hours before plugging with nickel corrosion product.<sup>5</sup> Attack of the Hastelloy N was uniform throughout the loop.

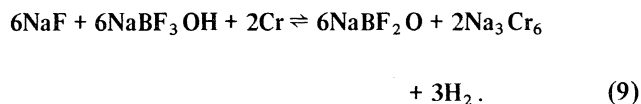
The hydroxide compound from Equation (5) may dissociate in the following manner



Combining Reactions (5), (6a), and (7) we get



Reactions (6a) and (7) can be combined to obtain



Removal of hydrogen from the system by diffusion through the metal would drive Reactions (8) and (9) to the right.

In another example, steam was injected into a Hastelloy N fluoroborate salt loop system, and very large initial weight changes (> 10 mpy) ensured.<sup>6</sup> The weight changes were temperature dependent in the manner of

Figures 3 through 7, with both losses and gains, and the attack was uniform. In time, and with no additional steam added to the system, the rate of corrosion decreased. Deposits in the cold section were mostly nickel and molybdenum.

In the above examples the strong oxidants reacted not only with the chromium and iron, but also with the ordinarily stable nickel and molybdenum to form fluorides. Almost all of the nickel and molybdenum fluorides were reduced in the cold region; they deposited as metal, making up the largest part of the deposit. If the saturation solubility of the ionic fluoride compounds in the salt had been reached, the deposit would have been in the form of the compound (the usual form that causes plugging).

The stainless steel attack is an example of initial selective removal of chromium, with some removal of iron from the chromium depleted areas. Selective attack accompanied by void formation, with more than one alloying element removed under conditions of high corrosion rates, has been observed for Inconel 600 in chloride salts<sup>7</sup> and stainless steel in an NaBF<sub>4</sub>-NaF system.<sup>8</sup>

The formation of subsurface voids is initiated by the oxidation of chromium along exposed surfaces through oxidation reduction reactions with impurities or constituents of the molten fluoride mixture. As the surface is depleted in chromium, chromium from the interior diffuses down the concentration gradient to the surface. Since diffusion occurs by a vacancy process, and in this particular situation is essentially monodirectional, an excess number of vacancies can be built up in the metal. These precipitate in areas of disregistry, principally at grain boundaries and impurities, to form voids. These voids tend to agglomerate and grow with increasing time, temperature, or both. Examinations have demonstrated that the subsurface voids are not connected with each other or with the surface. Voids of this same type have been developed in Inconel 600 by high temperature oxidation tests and high temperature vacuum tests, in which chromium is selectively removed.<sup>9</sup> Voids similar to these have also been developed in copper-brass diffusion couples and by the dezincification of brass.<sup>10</sup> All of these phenomena arise from the so-called Kirkendall effect, in which solute atoms of a given type diffuse out faster than other atoms from the crystal lattice can diffuse in to fill the resulting vacancies.

From the knowledge of the free energy of formation of various fluorides, one would expect, on a thermodynamic basis, that an alloy such as Hastelloy N, consisting mostly of nickel and molybdenum, is more noble than stainless steel, which is made up mostly of iron and chromium. These experiments show that the stainless steel is less resistant to fluoride salt corrosion and mass transfer than the Hastelloy N. Similarly, the titanium modified Hastelloy N with no iron is apparently more noble and corrosion resistant than the standard Hastelloy N with 5% Fe, and likewise the maraging steel with less chromium but more nickel than the Type 304L stainless steel is more noble and corrosion resistant. Kinetic behavior was controlled by the solid state diffusion of chromium in the alloy in systems where mass transfer was small and the apparent impurity content of the salt was low. In other systems, movement of more than chromium was involved. Predictions of the exact

behavior is yet a function of impurity content in the salt, small additions to the alloy, and temperature.

### Conclusions

1. Corrosion in the molten salt system of this experiment was manifested by temperature gradient mass transfer: loss of material from the hot zone and deposits in the cold zone.

2. Temperature gradient mass transfer in a Hastelloy N system containing  $\text{LiF-BeF}_2$  base salt is quite small (maximum corrosion rate of 0.1 mpy at 704 C) and usually involves only chromium; the process is controlled by the solid state diffusion of chromium in the alloy.

3. A titanium modified Hastelloy N, which contains no iron, showed smaller weight changes than the standard Hastelloy N, which contains 5% Fe.

4. Temperature gradient mass transfer of Type 304L stainless steel in  $\text{LiF-BeF}_2$  base salt involves the movement of both chromium and iron, with a corrosion rate of 1.1 mpy at 688 C. The process appears to be initially selective with respect to chromium and results in the formation of large voids.

5. The corrosion rate of the maraging steel, which is iron base with less chromium than stainless steel, is half that of the stainless steel.

6. In Hastelloy N with impure  $\text{NaBF}_4\text{-NaF}$  temperature gradient mass transfer of all the alloying elements of the alloy was observed. Nickel and molybdenum, which form the least stable fluorides, made up most of the deposit in the cold leg. The corrosion rate at the highest temperature, 607 C, was 0.6 mpy.

### Acknowledgments

It is a pleasure to acknowledge that E. J. Lawrence

supervised construction and operation of the thermal convection loops and was responsible for the weight change measurements. The author is also indebted to H. E. McCoy, Jr., J. H. DeVan, and T. S. Lundy for constructive review of the manuscript. Special thanks are extended to the Metallurgy group, especially C. E. Zachary, H. V. Mateer, T. J. Henson, and R. S. Crouse, the Analytical Chemistry Division, the Graphic Arts Department, B. Seivers of the Reactor Division, the Metals and Ceramics Division Reports Office for preparation of the manuscript, and particularly S. Peterson for invaluable assistance.

### References

1. *Fluid Fuel Reactors*, ed. by J. A. Lane, H. G. MacPherson, and F. Maslan, Addison-Wesley, Reading, Mass, 595 (1958).
2. L. S. Darken and R. W. Gurry, *Physical Chemistry of Metals*, McGraw-Hill, New York, p 445 (1953).
3. R. B. Evans, J. H. DeVan, and G. M. Watson, *Self-Diffusion of Chromium in Nickel Base Alloys*, ORNL-2982 (1961) January.
4. A. Glassner, *The Thermochemical Properties of the Oxides, Fluorides, and Chlorides to 2500 K*, ANL-5750 (1957).
5. *MSR Program Semiannu. Progr. Rept. Feb. 28, 1962*, ORNL-3282, p 72.
6. *MSR Program Semiannu. Progr. Rept. Aug. 31, 1969*, ORNL-4449, p 200-201.
7. R. Bakish and F. Kern, *Selective Corrosion of Inconel*, *Corrosion*, **16**, 553 (1960).
8. J. W. Koger and A. P. Litman, *Catastrophic Corrosion of Type 304 Stainless Steel in a System Circulating Fused Sodium Fluoroborate*, ORNL-TM-2741 (1970) January.
9. A. deS. Brasunas, *Sub-surface Porosity Developed in Sound Metals During High Temperature Corrosion*, *Met Progr.*, **62**, 88 (1952).
10. R. W. Balluffi and B. H. Alexander, *Development of Porosity by Unequal Diffusion in Substitutional Solutions*, SEP-83, Sylvania Electric Products (1952) February.